

## Corrosion behavior of Metallic Materials in Chicken Fat-Based Biodiesel

C.I. Rocabrundo-Valdés<sup>1,2</sup>, J.A. Hernández<sup>1</sup>, R. Muñoz-Ledo<sup>3</sup>, V.M. Salinas-Bravo<sup>3</sup>,  
M.A. Lucio-García<sup>4</sup>, R. Lopez-Sesenes<sup>5</sup>, J. Porcayo-Calderon<sup>1</sup>, J.G. González-Rodríguez<sup>1\*</sup>,

<sup>1</sup> Universidad Autónoma del Estado de Morelos, CIICAp. Av. Universidad No. 1001, Col. Chamilpa, Cuernavaca, Morelos, Mexico. C.P. 62209.

<sup>2</sup> Centro Nacional de Investigación y Desarrollo Tecnológico, Reforma 106, Temixco, Morelos, México.

<sup>3</sup> Instituto Nacional de Electricidad y Energías Limpias, Reforma 108, Temixco, Morelos, México.

<sup>4</sup> Universidad Autónoma de Yucatan, Fac. de Química, Merida, Yucatan, Mexico.

<sup>5</sup> Universidad Autónoma del Estado de Morelos, FCQI, Av. Universidad No. 1001, Col. Chamilpa, Cuernavaca, Morelos, Mexico. C.P. 62209.

\*E-mail: [ggonzalez@uaem.mx](mailto:ggonzalez@uaem.mx)

Received: 25 July 2019 / Accepted: 5 September 2019 / Published: 30 November 2019

---

The corrosion behaviour of 304 type stainless steel, 1018 carbon steel pure Al and Cu in a chicken fat-based biodiesel during 180 days has been studied by using electrochemical impedance spectroscopy and electrochemical noise measurements. Cu and carbon steel had the highest corrosion rate. Both Al and 304 type stainless exhibited a localised, whereas Cu and carbon steel a mixed type of corrosion. Corrosion process was under charge transfer control for short exposure times, but under adsorption/desorption control for longer exposure times. The corrosiveness of the biodiesel resulted from a degradation in its physicochemical properties.

---

**Keywords:** Chicken fat biodiesel, corrosion, electrochemical techniques.

### 1. INTRODUCTION

The increasing in energy demand due to a world growing population is causing the decrease in fossil fuels which can also cause environmental pollution. Due to this, extensive research work is being carried out looking for alternative sustainable fuels which satisfy the above mentioned demands. Biodiesel is an alternative fuel that can meet these characteristics [1]. Normally biodiesel is comprised of alkyl esters of fatty acids derived from renewable feed stock such as vegetable oil and animal fat. However, most of the biodiesel produced in the world comes from vegetable oils such as soybean oil, milkweed seed oil, *Jatropha curcas*, palm oil, sunflower and castor oil [2-9] etc. The residual oil left in

the fast food industry are also being investigated as a source of biodiesel as well [10]. However, very little research has been done on the possible use of animal fat as a possible source of biodiesel.

One of the main concerns of the use of biodiesel is the corrosion problems associated with metallic materials used in automobiles which are in contact with it such as fuel tank, fuel pumps, fuel feed pump, fuel lines, fuel injector, pistons, exhaust system, etc... [11-19]. The corrosion behavior of every material used in a biodiesel is different for the different biodiesels. For instance Kaul et al. [20] studied the corrosion behavior of Aluminum in different biodiesels obtained from *Jatropha Curcas*, *Karanja*, *Mahua* and *Salvadora*, finding that the biodiesel obtained from *Jatropha Curcas* was the most corrosive, whereas the least aggressive was the biodiesel obtained from *Salvadora*. Similarly, different metals have different corrosion behavior in the same biodiesel. Thus, in a research work where different metallic materials were corroded in palm biodiesel, the corrosion rate of aluminum was lower than the corrosion rate of copper and brass [21]. In a similar way, Hu et al. [22] evaluated the corrosion behavior of different metals used in automobiles such as aluminum (Al), copper (Cu), 304 type stainless steel (304 SS) and 1018 carbon steel (1018 CS) in a biodiesel obtained from rapeseed oil and methanol, finding that Cu had the highest corrosion rate followed by 1018 CS, whereas the most corrosion resistant was 304 SS. Thus, the goal of this research work is to evaluate the corrosion behavior of Al, Cu, 1018 CS and 304 SS in a biodiesel obtained from an animal fat, i.e. chicken.

## 2. EXPERIMENTAL PROCEDURE.

### 2.1. Synthesis of Biodiesel.

The synthesis process begins by heating the chicken fat at 50 °C during 24 hours. After this, it is filtered. A solution consisting of dissolving 5 g of KOH in 200 ml methanol is prepared, which is added to the filtered obtained chicken fat, heated at 50°C under stirred conditions during 10 minutes. After this, the obtained product is left during 20 hours, and then decanted.

### 2.2. Biodiesel characterization.

Chemical characterization of the obtained biodiesel including its density, viscosity, water contents, acid value and Gas Chromatography mass spectroscopy was carried out as described elsewhere [23].

### 2.3. Electrochemical measurements.

Electrochemical techniques electrochemical noise (EN) and the electrochemical impedance spectroscopy measurements (EIS). A ZRA ammeter from ACM Instruments was used in the EN measurements, which were carried out in a three electrode cell, where the graphite was used as the auxiliary electrode,  $Cl^-(4M)/Hg_2Cl_2(s)/Hg(l)/Pt$  as reference electrode and aluminum (Al), copper (Cu), 1018 carbon steel (1018CS) and 304 stainless steel (304SS) bars, encapsulated in a polymeric resin with

a surface area of  $0.32 \text{ cm}^2$ , were used as working electrodes. Prior to their immersion in biodiesel during a period of 180 days at room temperature and static conditions, the metal bars were mirror polished. For the EN readings in both potential and current, these were taken in blocks of 1024 data, at a sampling rate of one reading/s. The noise in current readings were taken by using a nominally identical working electrode. Trend removal was applied by using a least square fitting method. The noise resistance value,  $R_n$ , was determined as the ratio of the potential noise standard deviation,  $\sigma_v$ , over the current noise standard deviation,  $\sigma_i$ . Finally, for the EIS measurements, a Gamry PCI4-300 Potentiostat/Galvanostat was used for the Electrochemical Impedance Spectroscopy (EIS) measurements in a frequency range of 0.05 - 20000 Hz, with a signal amplitude of 30 mV around the free corrosion potential value,  $E_{\text{corr}}$ .

#### 2.4. Surface characteristics.

Changes in surface morphology and the elemental composition of the corrosion products were investigated by a LEO 1450 Vp scanning electron microscopy (SEM) attached to an energy dispersive X-ray spectroscope (SEM/EDS). Corrosion products on the biodiesel exposed metal surface were also examined by using X-ray diffraction (XRD). The XRD patterns of the corroded samples were recorded by using a diffractometer (Model: D2 Phaser, Bruker) with a  $\text{Cu K}\alpha$  radiation ( $1.5406 \times 10^{-10} \text{ m}$  wavelength), operated at 30 kV/10 mA.

### 3. RESULTS AND DISCUSSION

#### 3.1 Open circuit potential (OCP).

The change in the open circuit potential value (OCP) as a function of time for the different metals exposed to the chicken fat biodiesel is shown in Fig. 1, where it can be seen that this value shifted to a more active values as time elapsed for all metals regardless of its chemical composition. This indicates that although at the beginning of the test the metal surface was covered by a kind of protective film and its reactivity was very low, this film became more porous as time elapsed, less adherent to the metal, with an increase in the corrosion rate. Depending upon the nature of these corrosion products, they can be protective or non-protective. Fazal et al. [14] reported  $\text{Fe}_2\text{O}_3$ ,  $\text{Fe}_2\text{O}_2\text{CO}_3$  and  $\text{Fe}(\text{OH})_3$  as the formed compounds on mild steel exposed to palm biodiesel included, whereas only  $\text{Al}(\text{OH})_3$  was reported to be found for Al and for Cu it was found  $\text{Cu}_2\text{O}$ ,  $\text{CuO}$ ,  $\text{Cu}(\text{OH})_2$  and  $\text{CuCO}_3$  [21]. Towards the end of the test, the most active OCP values were for Cu and 1018 carbon steel, whereas the noblest values were for Al.

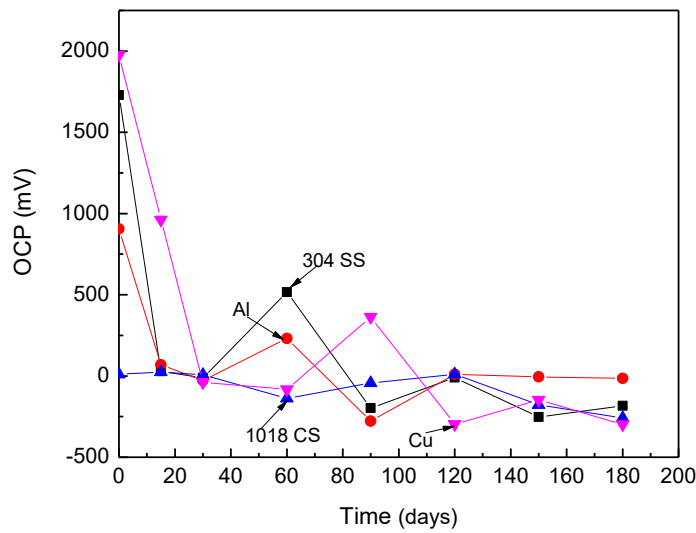


**Figure 1.** Variation in the open circuit potential value, OCP, for the different metals exposed to the chicken fat-based biodiesel.

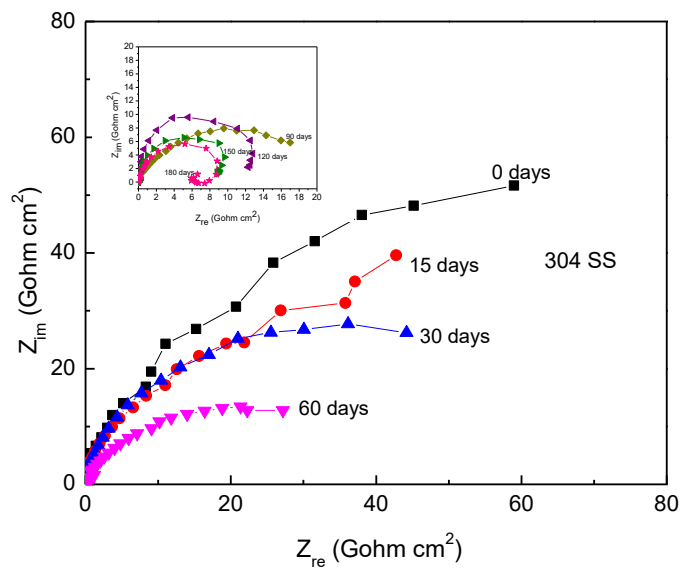


**Figure 2.** Nyquist diagrams for 304 type stainless steel at different exposure times to chicken fat-based biodiesel.

### 3.2 EIS measurements

Nyquist diagrams for the different metals exposed to chicken fat biodiesel as a function of the exposure time are shown in Figs. 2-5 respectively. It can be seen from these figures that regardless of the metal chemical composition data describe a single, depressed, capacitive semicircle at all frequency

values during the first 90-120 days of exposure to the biodiesel, indicating a charge transfer-controlled process.

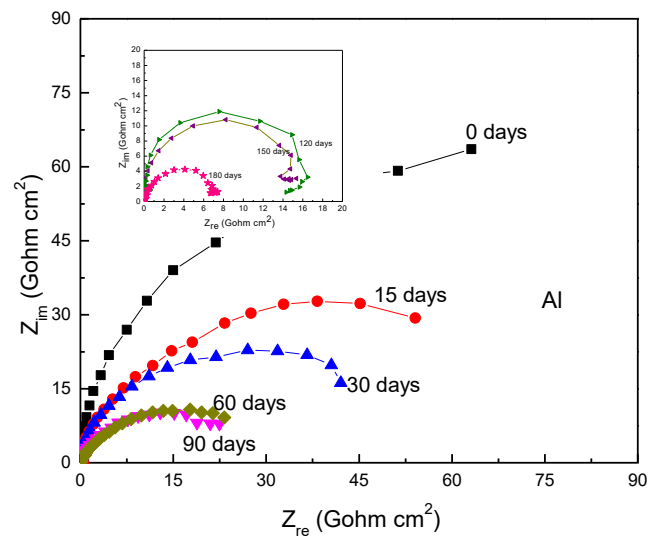


**Figure 3.** Nyquist diagrams for Al at different exposure times to chicken fat-based biodiesel.

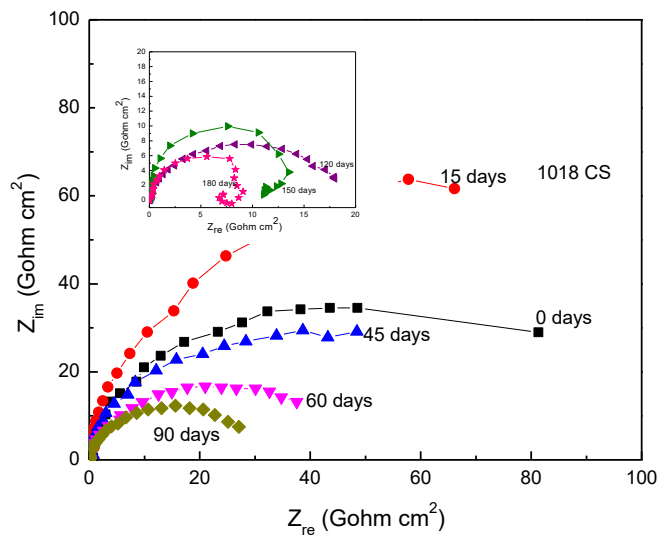


**Figure 4.** Nyquist diagrams for 1018 carbon steel at different exposure times to chicken fat-based biodiesel.

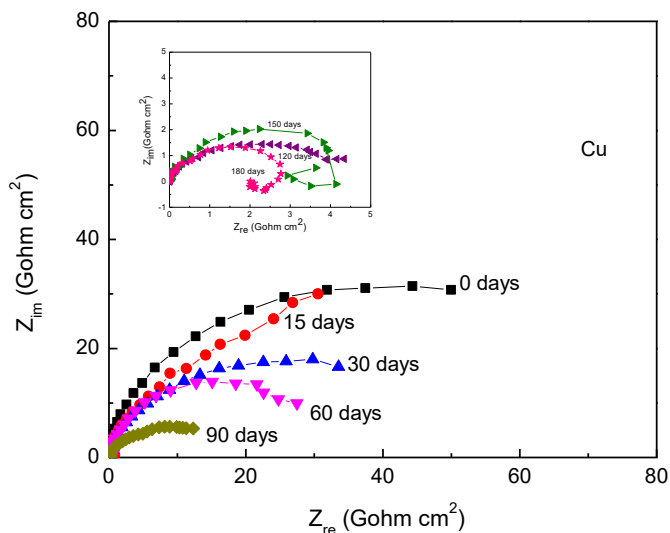


**Figure 5.** Nyquist diagrams for Cu at different exposure times to chicken fat-based biodiesel.

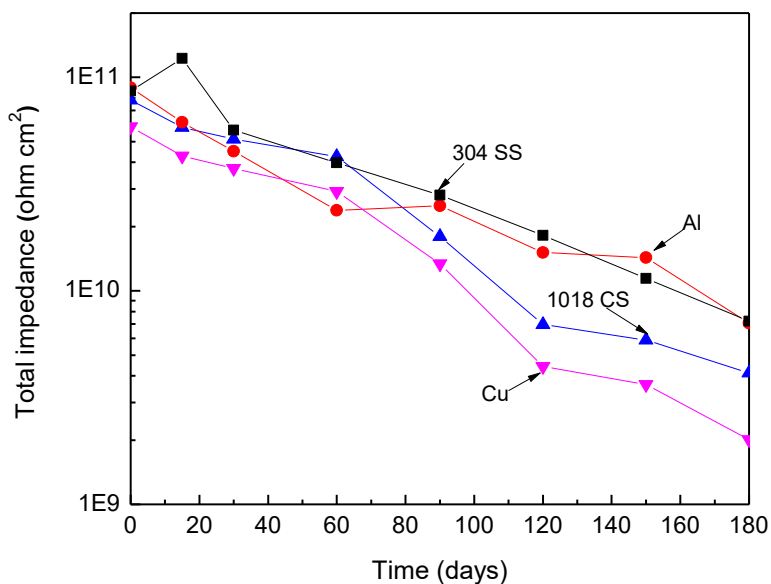


**Figure 6.** Change of the total impedance with exposure time for the different metals exposed to chicken fat-based biodiesel.

However, for times longer than 120 days or so, data describe a capacitive semicircle at high and intermediate frequency values, and a second inductive loop at lower frequency values, as reported for Al exposed to palm biodiesel [19], indicating a corrosion process controlled by a relaxation process due to the adsorption/desorption of species. The capacitive diameter corresponds to the charge transfer resistance,  $R_{ct}$ , equivalent to the polarization resistance,  $R_p$ , which is inversely proportional to the  $I_{corr}$

value, and it can be seen that for the different metals the  $R_{ct}$  value decreases as exposure time elapses, indicating an increase in the corrosion rate. This is more evident in Fig. 6 where the change in the total impedance as time elapses for the different metals is plotted. This plot clearly shows a decrease in the total impedance as the exposure time increases, indicating an increase in the corrosion rate. Additionally, as reported by some other works with the weight loss technique [12, 22], the metal with the highest corrosion rate when exposed to a rapeseed oil biodiesel was Cu followed by 1018 carbon steel, whereas the most corrosion resistant was 304 type stainless steel.

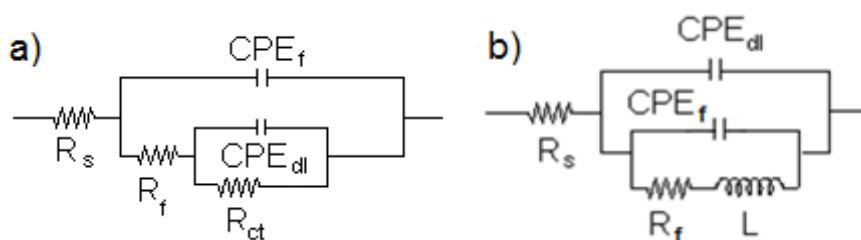


**Figure 7.** Equivalent circuits used to model EIS data a) during the first 120 hours, and b) times longer than 120 hours of exposure to chicken fat-based biodiesel.

**Table 1.** Electrochemical parameters used to simulate the EIS data of the different metals exposed to the chicken fat based biodiesel.

Metal	Day	$R_s$ ( $\Omega \text{ cm}^2$ )	$CPE_{dl}$ ( $\text{F/cm}^2$ )	$n_{dl}$	$R_{ct}$ ( $\Omega \text{ cm}^2$ )	$CPE_f$ ( $\text{F/cm}^2$ )	$n_f$	$R_f$ ( $\Omega \text{ cm}^2$ )	L ( $\text{H cm}^{-2}$ )
304 SS	0	$9.2 \times 10^5$	$1.6 \times 10^{-5}$	0.71	$9.9 \times 10^5$	$1.3 \times 10^{-10}$	0.98	$9.4 \times 10^{10}$	--
	180	$6.7 \times 10^3$	$2.4 \times 10^{-3}$	0.99	$4.9 \times 10^3$	$5.2 \times 10^{-10}$	0.49	$1.8 \times 10^9$	$3.4 \times 10^9$
Al	0	$3.3 \times 10^7$	$8.7 \times 10^{-7}$	0.78	$3.3 \times 10^7$	$2.7 \times 10^{-10}$	0.99	$5.9 \times 10^{10}$	--
	180	$2.8 \times 10^4$	$3.2 \times 10^{-7}$	0.99	$2.4 \times 10^9$	$8.4 \times 10^{-10}$	0.35	$6.2 \times 10^9$	$2.5 \times 10^9$
1018 CS	0	$1.9 \times 10^6$	$8.5 \times 10^{-6}$	0.52	$1.9 \times 10^6$	$1.0 \times 10^{-10}$	0.98	$8.0 \times 10^{10}$	--
	180	$3.6 \times 10^3$	$2.8 \times 10^{-9}$	0.99	$5.5 \times 10^9$	$2.6 \times 10^{-10}$	0.20	$3.8 \times 10^9$	$2.0 \times 10^9$
Cu	0	$7 \times 10^5$	$1.1 \times 10^{-5}$	0.42	$6.7 \times 10^5$	$2.1 \times 10^{-10}$	0.99	$7.0 \times 10^{10}$	--
	180	$4.1 \times 10^4$	$2.7 \times 10^{-8}$	0.99	$7.4 \times 10^8$	$3.1 \times 10^{-10}$	0.25	$1.6 \times 10^9$	$1.2 \times 10^9$

EIS data can be fitted by a combination of resistances, capacitors and inductances, i.e. Electric circuits as those given in Fig. 7 where the biodiesel resistance is given by  $R_s$ , the charge transfer resistance is represented by  $R_{ct}$ , the double layer capacitance by  $C_{dl}$ , the inductive element and its resistance by L and  $R_L$  respectively, the resistance of any formed film on to the surface metal and its capacitance by  $R_f$  and  $C_f$  [24]. However, to take into account heterogeneities on the metal surface which deviate the response from an ideal one, a constant phase element (CPE) is introduced to replace an ideal capacitor. The impedance of a CPE is described by the expression:

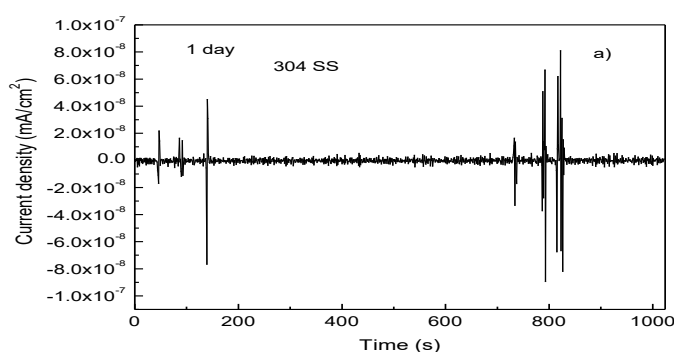
$$Z_{CPE} = Y^{-1} (i\omega)^{-n} \tag{3}$$

where  $Y$  is a proportional factor,  $i$  is  $\sqrt{-1}$ ,  $w$  is  $2\pi f$ ,  $f$  the frequency and  $n$  is a parameter that gives metals properties such as roughness [24]. Results for the first and last days of exposure to the biodiesel are given in table 1.

This table shows the high resistance value of the solution, which is normal for a biodiesel, however, this value decreases between 2 and 3 orders of magnitude towards the end of the tests, which implies an enhancing of the electrochemical processes, with an increase in the corrosion rate as time elapses. Another important feature to be noted, is that regardless of the metal chemical composition, the resistance of the corrosion products,  $R_f$ , is much higher than the charge transfer resistance,  $R_{ct}$ , indicating that the metal corrosion resistance is given by the film formed by the corrosion products. In addition to this, the  $CPE_f$  value increases as time elapses in all cases. We can explain this by taking in to account that the capacitance is proportional to the product of the film dielectric constant and the vacuum electrical permittivity and inversely proportional to the film thickness [25]. Thus, the increase in the capacitance or the  $CPE_f$  is due to an increase in the dielectric constant or to a decrease in the film thickness. Finally, at the beginning of the tests, when the corrosion rate is low, the metal surface roughness is low and the  $n_f$  value is close to 1.0, but as the corrosion rate increases, the metal surface becomes rougher with a decrease in the  $n_f$  value, approaching to a value of 0.5.

### 3.3 EN measurements

As a way of example, Fig. 8 shows atypical time series for the noise in current and in potential for 304 type stainless steel after 1 and 180 days of exposure to the chicken fat-based biodiesel. It can be seen that at the beginning of the test, time series consist of transients with low intensity and high frequency combined with some transients of much higher intensity but lower frequency, indicative of the rupture of any protective film and its re-building or metastable pitting type of corrosion [26]. As we have established above,  $Fe_2O_3$ ,  $Fe_2O_2CO_3$  and  $Fe(OH)_3$  were the compounds formed on to mild steel and  $Al(OH)_3$  on Al and  $Cu_2O$ ,  $CuO$ ,  $Cu(OH)_2$  and  $CuCO_3$  when Cu exposed to palm biodiesel [21]. Thus, the observed transients are due to the rupture of these films and to their repair. After 180 days of exposure to the biodiesel, the intensity of the observed transients has decreased considerably and time series consist mainly of transients with low intensity and high frequency, indicative of a metal undergoing a uniform type of corrosion.



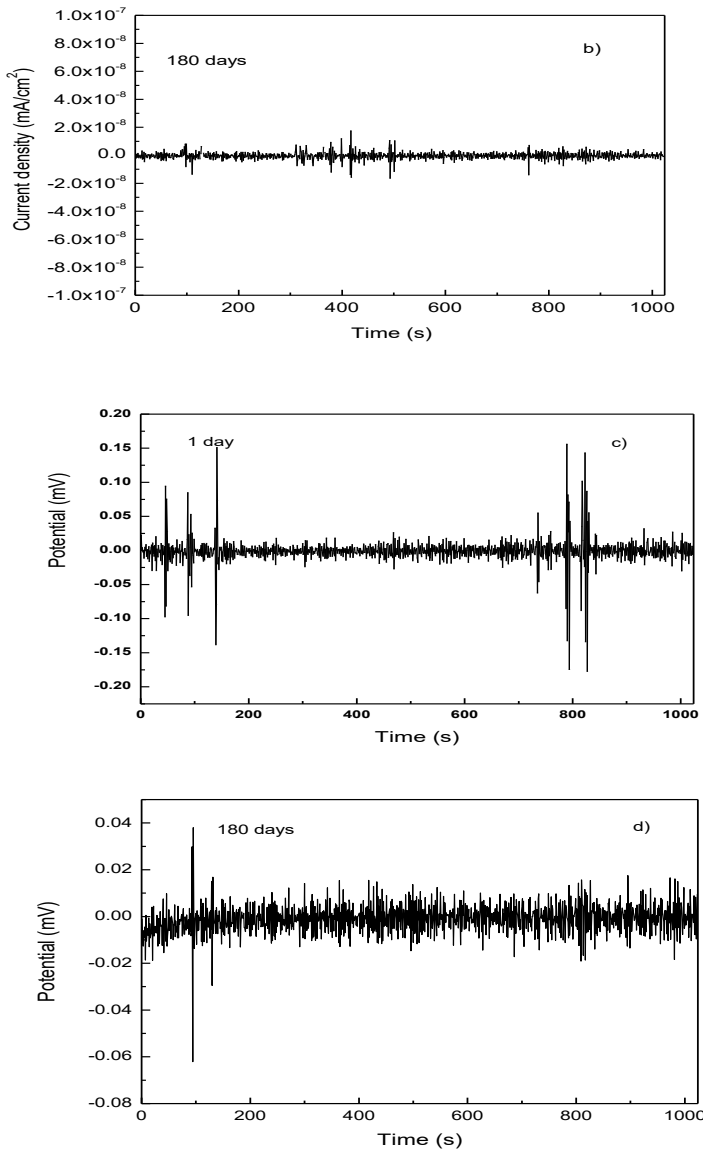


**Figure 8.** Electrochemical noise in current (a and b) and potential (c and d) after 1 and 180 days of exposure for 304 type stainless steel to chicken fat-based biodiesel.

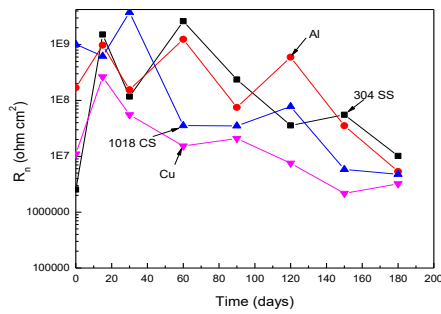


**Figure 9.** Change of the noise resistance value,  $R_n$ , with exposure time for the different metals exposed to chicken fat-based biodiesel.

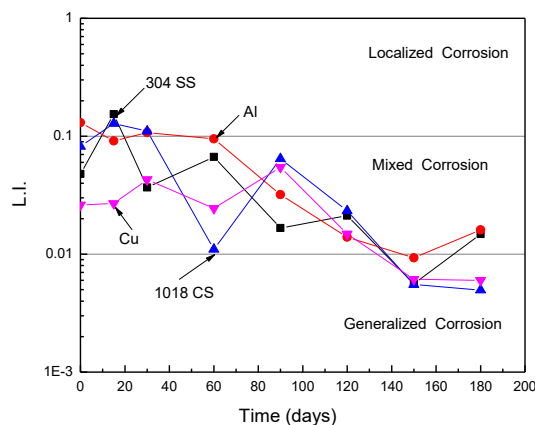


**Figure 10.** Change of the localization index value, L.I., with exposure time for the different metals exposed to the chicken fat-based biodiesel.

We can obtain a noise resistance value,  $R_n$ , by the ratio between  $\sigma_v$ , over  $\sigma_1$ , for the different metals exposed to the chicken fat-based biodiesel are given in Fig. 9. Although there is some scatter in the data, the general trend of the  $R_n$  value is to decrease as time elapses, similar to the trend exhibited by the total impedance shown in Fig. 6. Additionally, in a similar way to the total impedance data shown in Fig. 6, the highest  $R_n$  value was for Al and 304 type stainless steel, whereas the lowest values, and thus the highest corrosion rates, were exhibited by Cu. Thus, different techniques give similar results, which is very encouraging. However, it should be noticed that the total impedance values are up to 4 orders of magnitude higher than the  $R_n$  ones. Maybe this is because the total impedance values includes all the resistance values, including solution resistance (which are within the order of  $10^5$  ohm  $cm^2$ ), charge transfer resistance and the resistance of the corrosion products, which are related with uniform type of corrosion, whereas  $R_n$  is related with localized events.

In order to predict the type of corrosion that each metal is susceptible to, a parameter called Localization Index (L.I.) was calculated according to the following equation:

$$L.I. = \frac{\sigma_i}{i_{rms}} \tag{4}$$

where  $i_{rms}$  is the current root mean square value [27]. A metal is very susceptible to localized corrosion when the values for L.I. lie between 1 and 0.1, to a mixture of both uniform and localized corrosion when the values for L.I. values are between 0.1 and 0.01, and towards uniform corrosion when L.I. is between 0.01 and 0.001. Fig. 10 shows that during the first 120 hours of exposition, the metals are susceptible to a mixed type of corrosion, i.e. a mixture of localized and uniform type of corrosion, but towards the end of the tests, the 4 metals should be susceptible to generalized, uniform type of corrosion.

### 3.4 Analysis of corroded samples

Micrographs of corroded surface metals exposed to 180 days to the chicken fat-based biodiesel are shown in Fig. 11. where it can be seen that for 304 type stainless steel and Al, Fig. 10 a and b, a localized type of corrosion is the dominant type of corrosion although some incipient uniform type of corrosion is evident.

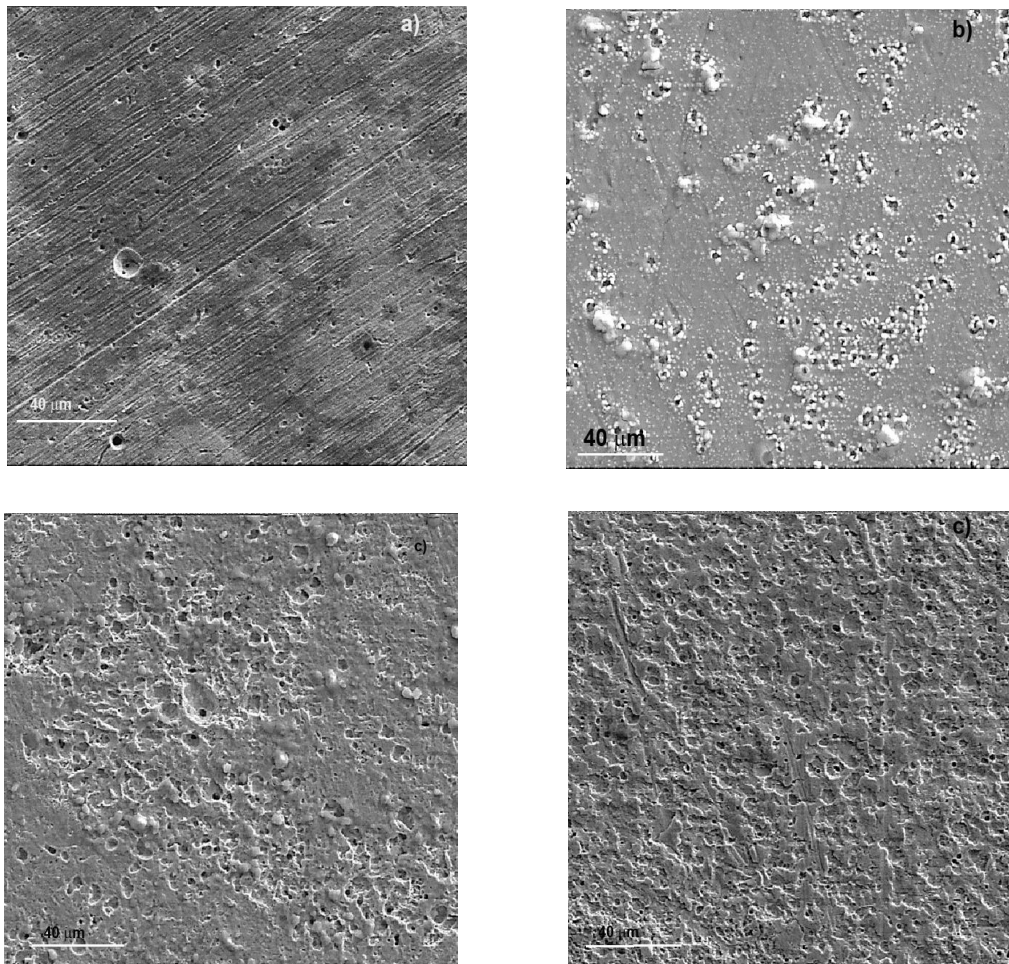


**Figure 11.** Micrographs of corroded surfaces for a) 304 type stainless steel, b) Al, c) 1018 carbon steel and d) Cu exposed to chicken fat-based biodiesel.

However, for 1018 carbon steel and pure Cu, Fig. 10 c and d, the dominant type of corrosion was uniform one, but some pits could be seen. It is evident from this figure, that the most damaged surface metal was Cu, followed by 1018 carbon steel, whereas the metals which were marginally corroded by the biodiesel were 304 type stainless steel and Al, as reported by some other workers [12, 22, 29]. X-ray patterns of the corrosion products found on top of the corroded metals are shown in Fig. 11. For 304 type stainless steel, only  $\text{Cr}_2\text{O}_3$  oxide was found, which is normally developed by stainless steels and it is the responsible for the great corrosion resistance of these steels [28]. For Al,  $\text{Al}_2\text{O}_3$  was detected,

which is also well known to be a very protective oxide, which provides a high corrosion resistance to Al and its alloys [30-32]. Thus, both  $\text{Cr}_2\text{O}_3$  and  $\text{Al}_2\text{O}_3$  oxides are responsible for the relatively high corrosion resistance of 304 type stainless steel and Al in chicken fat-base biodiesel. For 1018 carbon steel, it was found  $\text{Fe}(\text{OH})_2$  and  $\text{Fe}_2\text{O}_3$  whereas for Cu  $\text{Cu}(\text{OH})_2$ ,  $\text{Cu}(\text{CO}_3)_2$  and  $\text{Cu}_2\text{O}$  were detected, which, according to the presented results, did not bring a high corrosion protection for 1018 carbon steel and Cu exposed to chicken fat biodiesel. These results are similar to those reported in literature. Thus, Fazal et al. [14] found  $\text{Fe}_2\text{O}_3$ ,  $\text{Fe}_2\text{O}_2\text{CO}_3$  and  $\text{Fe}(\text{OH})_3$  for mild steel,  $\text{Al}(\text{OH})_3$  for Al and  $\text{Cu}_2\text{O}$ ,  $\text{CuO}$ ,  $\text{Cu}(\text{OH})_2$  and  $\text{CuCO}_3$  for Cu exposed to palm biodiesel [21]. The reason of why species such as  $\text{Cu}(\text{CO}_3)_2$  and  $\text{Cu}_2\text{O}$  were detected is very likely to be due to the absorbed water due to the hygroscopic nature of biodiesel [12],  $\text{O}_2$  and  $\text{CO}_2$  from the atmosphere [14].

### 3.5 Biodiesel composition.

Physicochemical properties of the obtained chicken fat biodiesel before and after being in contact with Al and 1018 carbon steel are given in table 2, where it can be seen that the density of the biodiesel remained practically unaltered during the corrosion test, however both kinematic viscosity and acidity increased in a considerable way whereas the water contents decreased after the corrosion test. As a standard, the maximum total acid number (TAN) for a biodiesel has been established as 0.80 mg KOH/g [33], higher than the reported in our case, 0.70 mg KOH/g, and it increases due to a oxidation of biodiesel whereas it is in service.

**Table 2.** Differences in physical-chemical properties of chicken fat biodiesel before and after exposure of aluminum and 1018 carbon steel at room temperature during 180 days.

Property	Before corrosion test	After corrosion test	
		Al	1018 CS
Density ( $\text{g}/\text{cm}^3$ )	0.8914	0.9033	0.9029
Kinematic viscosity (cSt)	9.0955	17.40	17.15
Acidity (mg KOH/g)	0.7	83.028	74.052
Water content (ppm)	7090	5000	4300

The TAN number is a parameter which provide an indication of the degree of the biodiesel oxidation for its contact with metals [20] with the formation of acids [34]. By exploring data on table 2, it is clear that the degree of TAN number increased after exposure to the different metals such as Al and 1018 carbon steel. However, the TAN number after the corrosion are extremely high as compared with those for carbon steel exposed to palm oil biodiesel where values lower than 2.0 were reported [14], which indicates that the chicken fat-based biodiesel is greatly oxidized. In a similar way to oxidation of biodiesel, the presence of water in the biodiesel will increase the biodiesel corrosiveness.

**Table 3.** GC-MS analysis showing compositional differences of the chicken fat biodiesel before and after exposure to aluminum and 1018 carbon steel during 180 days.

Name / Molecular Formula	% of Area		
	B100 Initial	B100/ Al	B100/ 1018CS
Methyl (Z)-tetradec-11-enoate C <sub>15</sub> H <sub>28</sub> O <sub>2</sub>	0.315	0.462	0.464
Methyl tetradecanoate C <sub>15</sub> H <sub>30</sub> O <sub>2</sub>	1.219	1.82	1.737
Methyl (7E,10E)-7,10-hexadecadienoate C <sub>17</sub> H <sub>30</sub> O <sub>2</sub>	0.252	0	0
Methyl (Z)-hexadec-9-enoate C <sub>17</sub> H <sub>32</sub> O <sub>2</sub>	9.72	11.328	11.058
Methyl hexadecanoate C <sub>17</sub> H <sub>34</sub> O <sub>2</sub>	24.787	26.66	26.638
Methyl heptadecanoate C <sub>18</sub> H <sub>36</sub> O <sub>2</sub>	0.238	0	0
Methyl (9Z,12Z)-octadeca-9,12-dienoate C <sub>19</sub> H <sub>34</sub> O <sub>2</sub>	9.397	3.722	3.595
Methyl (E)-octadec-9-enoate C <sub>19</sub> H <sub>36</sub> O <sub>2</sub>	17.139	0	0
Methyl (Z)-octadec-9-enoate C <sub>19</sub> H <sub>36</sub> O <sub>2</sub>	26.522	0	0
Methyl octadecanoate C <sub>19</sub> H <sub>38</sub> O <sub>2</sub>	8.425	10.433	10.564
Methyl (5Z,8Z,11Z,14Z)-icosa-5,8,11,14-tetraenoate C <sub>21</sub> H <sub>34</sub> O <sub>2</sub>	0.313	0	0
Methyl (7E,10E,13E)-icosa-7,10,13-trienoate C <sub>21</sub> H <sub>36</sub> O <sub>2</sub>	0.35	0	0
Methyl (10E,13E)-10,13-icosadienoate C <sub>21</sub> H <sub>38</sub> O <sub>2</sub>	0.408	0	0
Methyl (E)-icos-11-enoate C <sub>21</sub> H <sub>40</sub> O <sub>2</sub>	0.688	1.65	1.516
Methyl icosanoate C <sub>21</sub> H <sub>42</sub> O <sub>2</sub>	0.227	0.301	0
Methyl octanoate C <sub>9</sub> H <sub>18</sub> O <sub>2</sub> (C8:0)	0	0.528	0.558
(2E,4E)-deca-2,4-dienal C <sub>10</sub> H <sub>16</sub> O	0	0.516	0.539
Methyl 9-oxononanoate C <sub>10</sub> H <sub>18</sub> O <sub>3</sub>	0	1.597	1.531
Methyl 8-[2-[[2-[(2-ethylcyclopropyl)methyl]cyclopropyl]methyl]cyclopropyl]octanoate C <sub>22</sub> H <sub>38</sub> O <sub>2</sub>	0	0.545	0
Methyl (Z)-octadec-11-enoate C <sub>19</sub> H <sub>36</sub> O <sub>2</sub>	0	40.02	40.733
Methyl 8-[(2R,3R)-3-octyloxiran-2-yl]octanoate C <sub>19</sub> H <sub>36</sub> O <sub>3</sub>	0	0.418	0
Methyl 8-[(2S,3R)-3-octyloxiran-2-yl]octanoate C <sub>19</sub> H <sub>36</sub> O <sub>3</sub>	0	0	0.378
Bis(2-ethylhexyl) benzene-1,2-dicarboxylate C <sub>24</sub> H <sub>38</sub> O <sub>4</sub>	0	0	0.69

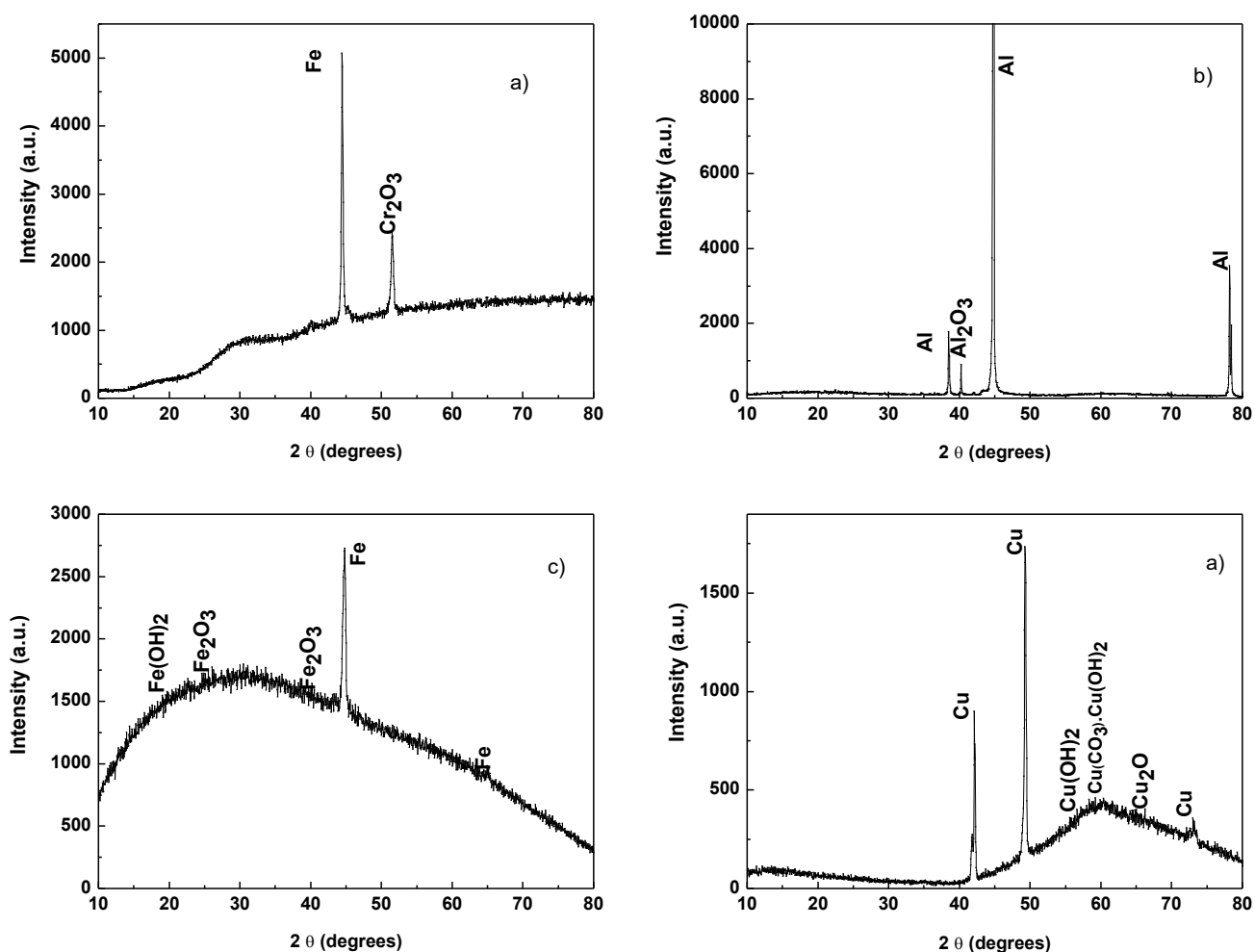


**Figure 12.** XRD patterns of the corrosion products found on top of a) 304 type stainless steel, b) Al, c) 1018 carbon steel and d) Cu exposed to chicken fat-based biodiesel.

Analysis of compositional change of chicken biodiesel before and after its exposure to metallic surfaces, table 3, shows that some components disappear or appear in a lower amount and some others appear after being in contact with the different metals. Some of the major reduction with respect to the initial condition corresponds to the methyl esters with a greater number of unsaturations, like Methyl (7E,10E)-7,10-hexadecadienoate (from 0.252% to 0%), Methyl heptadecanoate (from 0.238% to 0%), Methyl (9Z,12Z)-octadeca-9,12-dienoate (from 9.397% to 3.722%), Methyl (10E,13E)-10,13-icosadienoate (from 0.408% to 0%), Methyl (7E,10E,13E)-icosa-7,10,13-trienoate (from 0.35% to 0%) Methyl (5Z,8Z,11Z,14Z)-icosa-5,8,11,14-tetraenoate (from 0.313% to 0%). This may be a consequence of reactions resulting from the contact with metals or the absorption of O<sub>2</sub> and CO<sub>2</sub> from moisture. Different types of compounds like short chain esters (methyl octanoate and methyl 9-oxononanoate),

unsaturated aldehydes, (2E,4E)-deca-2,4-dienal; diester (bis(2-ethylhexyl) benzene-1,2-dicarboxylate) and other such as methyl 8-[2-[[2-[(2-ethylcyclopropyl)methyl]cyclopropyl]methyl]cyclopropyl]octanoate, methyl 8-[(2R,3R)-3-octyloxiran-2-yl]octanoate and methyl 8-[(2S,3R)-3-octyloxiran-2-yl]octanoate are produced after exposure of biodiesel to metal. This is in agreement with previous studies on the effect of water, O<sub>2</sub>, methanol, free glycerol, free fatty acids, impurities, metals in contact, etc., on the degradation of saturated and unsaturated compounds of biodiesel [14, 15, 17, 21].

Absorbed water from the environment can react with esters to convert them back to fatty acids such as formic, caproic, acetic and propionic acids, increasing the biodiesel corrosiveness [35]. It has been reported [33] that metals such as copper, brass, lead and zinc accelerate the oxidation of biodiesel increasing their corrosion rates. In addition to increase the biodiesel corrosiveness, these compositional changes can degrade the properties of the biofuel as reported in table 2.

#### 4. CONCLUSIONS

Corrosion behavior of 304 type stainless steel, Al, 1018 carbon steel and Cu in a chicken fat-based biodiesel has been studied. Results have shown that corrosion rate increases with exposure time. Metals with the highest corrosion rates were Cu and carbon steel, whereas Al and 304 type stainless steel exhibited the lowest corrosion rate. Pure Al and 304 type stainless steel exhibited mainly a localized type of corrosion such as pitting, whereas Cu and carbon steel exhibited a mixed type of corrosion. Corrosion process was under a charge control for all metals during the first 120 days of exposure, but it was controlled by an adsorption/desorption process for longer times than this. The corrosiveness of the chicken fat-based biodiesel is due to its oxidation for its contact with the different metals, increasing the TAN number, viscosity, and by forming new aggressive compounds.

#### References

1. J. Villarreal-Castellon, F.E. Mercader-Trejo, A. Álvarez-López, E.R. Larios-Durán, R. Antaño-López, R. Herrera-Basurto, A. Chacón-López, A. Rodríguez-López and U. López-García, *Int. J. Electrochem. Sci.*, 13 (2018) 5452.
2. N. Dizge and B. Keskinler, *Biomass Bioenergy*, 32 (2008) 1274.
3. M. Canakci and H. Sanli, *J. Ind. Microbiol. Biotechnol.*, 35 (2008) 431.
4. R.A. Holser and R. Harry-O’Kuru, *Fuel*, 85 (2006) 2106.
5. S. Fernando, P. Karra, R. Hernande and S. J. Kumar, *Energy*, 32 (2007) 844.
6. U. Rashid, F. Anwar, R.M. Bryan and G. Knothe, *Bioresour. Technol.*, 99 (2008) 8175.
7. Tina R. C. Zezza, Leonardo L. Paim, and Nelson R. Stradiotto, *Int. J. Electrochem. Sci.*, 8 (2013) 658.
8. M.A. Kalam and H.H. Masjuki, *Biomass and Bioenergy*, 23 (2002) 471.
9. Z. Ilham and S. Saka, *Bioresour Technol.*, 101 (2010) 2735.
10. M. Canakci, *Bioresour Technol.*, 11 (2005) 1.
11. A. S. M. A. Haseeb, M. A. Fazal, M. I. Jahirul and H. H. Masjuki, *Fuel*, 90 (2011) 922.
12. A. S. M. A. Haseeb, H. H. Masjuki, L. J. Ann and M. A. Fazal, *Fuel Process. Technol.*, 91 (2010)

329.

13. A. Sarin, R. Arora, N. P. Singh, M. Sharma and R. K. Malhotra, *Energy*, 34 (2009) 1271.
14. M. A. Fazal, A. S. M. A. Haseeb and H. H. Masjuki, *Energy*, 36 (2011) 3328.
15. A. S. M. A. Haseeb, S. Y. Sia, M. A. Fazal and H. H. Masjuki, *Energy*, 35 (2010) 1460.
16. S. Fernando, P. Karra, R. Hernandez and S. K. Jha, *Energy*, 32 (2007) 844.
17. M. R. Jakeria, M. A. Fazal and A. S. M. A. Haseeb, *Renew. Sustain. Energy Rev.*, 30 (2014) 154.
18. S. Kaul, R. C. Saxena, A. Kumar, M. S. Negi, A. K. Bhatnagar, H. B. Goyal and A. K. Gupta, *Fuel Process. Technol.*, 88 (2007) 303.
19. L. Díaz-Ballote, J. F. López-Sansores, L. Maldonado-López and L. F. Garfias-Mesias, *Electrochem. Commun.*, 11 (2009) 41.
20. S. Kaul, R.C. Saxena, A. Kumar, M.S. Negi, A.K. Bhatnagar and H. Goyal, *Fuel Process Technol.*, 88 (2007) 303.
21. M. A. Fazal, A. S. M. A. Haseeb and H. H. Masjuki, *Energy*, 40 (2012) 76.
22. Enzhu Hu, Yufu Xu, Xianguo Hu, Lijun Pan and Shaotong Jiang, *Renewable Energy*, 37 (2012) 371.
23. C. I. Rocabruno-Valdés, J. A. Hernández, A. U. Juantorena, E. G. Arenas, R. Lopez-Sesenes, V. M. Salinas-Bravo and J. G. González-Rodríguez, *Corr. Eng. Sci. Technol.* 53 (2018) 253.
24. E.A.M. Hussain and M.J. Robinson, *Corros. Sci.*, 49 (2007) 1737.
25. E. Poorqasemi, O. Abootalebi, M. Peikari and F. Haqdar, *Corros. Sci.*, 51 (2009) 1043.
26. K. Hladky and J.L. Dawson, *Corros. Sci.*, 22 (1982) 231.
27. H.H. Huang, W.T. Tsay and J.T. Lee, *Corrosion*, 52 (1996) 708.
28. J.A. Sedricks, *Corrosion of Stainless Steels*, John Wiley and Sons, 1979, New Jersey, U.S.A.
29. D.P. Geller, T.T. Adams and J.W. Goodrum, *Fuel*, 87 (2008) 92.
30. O.K. Abiola and J.O.E. Otaigbe, *Corros. Sci.*, 50 (2008) 242.
31. A.R. Yazdzad, T. Shahrabi and M.G. Hosseini, *Mater. Chem. Phys.*, 109 (2008) 199.
32. M.L. Doche, J.J. Rameau, R. Durand and F. Novel-Cattin, *Corros. Sci.*, 41 (1999) 805.
33. ASTM International (ASTM, 1994f, ASTM, 1994j). Standard specification for biodiesel fuel – blend stock (B100) for distillate fuels; 2002.
34. K. Yamane, K. Kawasaki, K. Sone, T. Hara and T. Prakoso, *Int. J. Eng. Res.*, 8 (2007) 307.
35. X.Y. Lou and P.M. Singh, *Corros. Sci.*, 52 (2010) 2303.

© 2020 The Authors. Published by ESG ([www.electrochemsci.org](http://www.electrochemsci.org)). This article is an open access article distributed under the terms and conditions of the Creative Commons Attribution license (<http://creativecommons.org/licenses/by/4.0/>).